

HLS-Seek: QoR-Aware Code Generation for High-Level Synthesis via Proxy Comparative Reward Reinforcement Learning

Qingyun Zou
National University of Singapore
Singapore, Singapore

Feng Yu
National University of Singapore
Singapore, Singapore

Hongshi Tan
National University of Singapore
Singapore, Singapore

Yao Chen
National University of Singapore
Singapore, Singapore

Bingsheng He
National University of Singapore
Singapore, Singapore

Weng-fai Wong
National University of Singapore
Singapore, Singapore

Abstract

High-Level Synthesis (HLS) compiles algorithmic C/C++ descriptions into hardware, with Quality of Results (QoR)—latency and resource utilization—critically governed by pragma configurations and code structure. Existing LLM-based HLS approaches train for functional correctness but ignore QoR entirely. We observe that reinforcement learning (RL) for HLS does not require absolute synthesis results—only relative comparisons between candidates. Based on this insight, we propose **HLS-Seek**, a QoR-aware NL-to-HLS framework that replaces expensive synthesis-in-the-loop RL with a comparative proxy reward model achieving 99.53% Pareto-dominance accuracy. To prevent reward hacking, we introduce *uncertainty-aware Monte Carlo (MC) dropout switching* that selectively invokes real Vitis HLS synthesis for low-confidence candidates and online updates the proxy, creating a self-improving reward system. HLS-Seek achieves 81.5% syntax correctness pass@1 and 81.4% Func@5 on HLS-eval with only 7B parameters, surpassing GPT-5.1 and other frontier models while achieving 8.5× faster training than real-reward RL. On QoR evaluation, HLS-Seek achieves the lowest latency on 16/30 kernels and Pareto-dominates HLS-specific baselines on 9 kernels.

CCS Concepts

- Hardware → High-level and register-transfer level synthesis.

Keywords

HLS code generation, reinforcement learning, quality of results, large language models

1 Introduction

High-Level Synthesis (HLS) compiles algorithmic C/C++ descriptions into Register Transfer Level (RTL) hardware implementations, and has become a widely adopted methodology for rapid prototyping across diverse domains, including machine learning accelerators [5, 8, 28], graph processing engines [4, 7, 26], and data-intensive applications [1, 15, 18], on both Field-Programmable Gate Array (FPGA) and Application-Specific Integrated Circuit (ASIC) platforms [14, 20, 22].

Recently, there has been growing interest in leveraging large language models (LLMs) to automate HLS code generation from high-level specifications [9, 16, 21, 23, 24]. For example, Gai et al. [9]

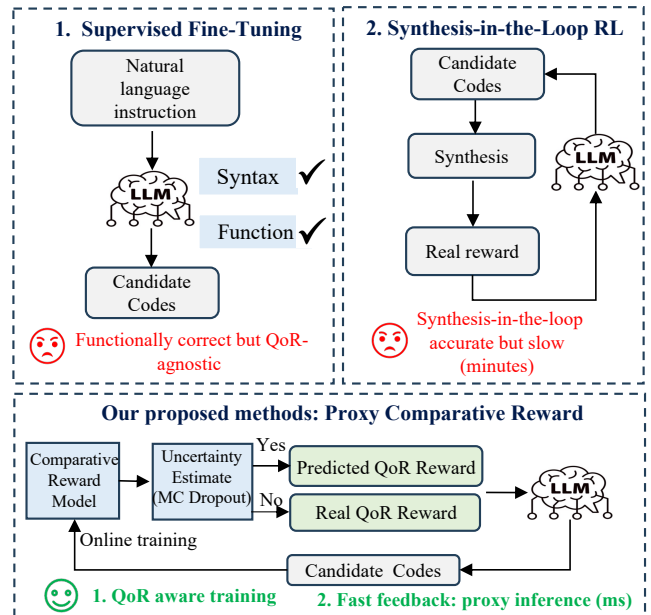


Figure 1: Three training methods for LLM-based HLS code generation.

fine-tune CodeLlama on HLS benchmarks for functional correctness, and SAGE-HLS [16] incorporates AST-guided representations to improve code structure awareness, demonstrating that LLMs can generate synthesizable hardware code with increasing reliability. These efforts highlight the potential of LLMs to significantly improve developer productivity and lower the barrier to hardware design.

However, these approaches primarily aim to generate runnable kernels, while the Quality of Results (QoR), which is critical for real-world accelerator deployment [14], is largely overlooked. QoR reflects low-level hardware performance and efficiency, and is typically measured by execution latency and resource utilization, including LUTs, DSPs, BRAMs, and FFs. It is determined by the microarchitectural structure of the kernel, the pragma configurations and code optimizations applied in the HLS compilation flow, as well as hardware resource instantiation behavior and downstream physical implementation optimizations [14]. As a result, QoR cannot be

accurately inferred from software code analysis alone and instead requires evaluation through the synthesis and implementation.

As shown in Figure 1, existing training paradigms face limitations for QoR-aware HLS generation. Supervised Fine-Tuning (SFT)-based approaches [9, 16] produce functionally correct code but are QoR-agnostic—all compilable designs receive equal training signal regardless of hardware performance. In the RTL domain, ChipSeek-R1 [6] demonstrates that real synthesis feedback can serve as an effective Reinforcement Learning (RL) reward. However, extending this synthesis-in-the-loop paradigm to HLS is prohibitively expensive: each HLS synthesis run takes minutes to hours (e.g., ThunderGP [4]), and RL training requires over 12,500 evaluations, making it infeasible at scale.

To overcome this bottleneck, we observe a key insight: *RL training does not require absolute QoR values from synthesis—only relative comparisons between candidates*. Knowing which of two designs is better suffices for policy improvement via group-relative advantage estimation, without needing exact latency or resource numbers. This motivates us to train a lightweight *comparative reward model* that predicts, given two candidate HLS designs, which achieves a better resource-latency trade-off—achieving 99.53% dominance accuracy and 99.42% latency accuracy without invoking synthesis. To safeguard against reward hacking as the RL policy explores out-of-distribution pragma configurations, the reward model estimates its own confidence via MC dropout and selectively falls back to real Vitis HLS synthesis for high-uncertainty candidates. Crucially, these synthesis results are fed back to *online update* the reward model, continuously expanding its coverage. This self-improving mechanism reduces the synthesis trigger rate over the course of training, keeping overall cost close to a proxy-only baseline while maintaining reward fidelity.

Based on this reward design, we propose **HLS-Seek**, a QoR-aware NL-to-HLS code generation framework trained in three stages. To address training data scarcity, we build upon the open-source dataset and apply a novel *Pareto-Proximal Quality-Diversity Sampling* strategy to curate QoR-competitive HLS implementations from its DSE results. We further leverage commercial reasoning models to generate chain-of-thought *reasoning traces*, step-by-step rationales for code optimization. Training then proceeds as: (i) diversity-oriented SFT on a broad HLS corpus with QoR descriptions, exposing the model to diverse pragma configurations; (ii) cold-start SFT on Pareto-proximal data with reasoning traces, instilling hardware reasoning capability before RL; and (iii) Group Relative Policy Optimization (GRPO) [25] with a four-component reward—reasoning format, compilation, functional correctness, and predicted QoR from the comparative reward model. Our main contributions are:

- We identify that RL for HLS code generation requires only relative QoR signals, not absolute synthesis results. Based on this insight, we propose a comparative proxy reward model with uncertainty-aware MC dropout switching that provides fast, accurate, and self-improving reward feedback during GRPO training.
- We present **HLS-Seek**¹, a complete QoR-aware NL-to-HLS framework comprising: a three-stage training pipeline (diversity SFT → cold-start SFT with reasoning traces → proxy reward GRPO),

Table 1: Comparison of LLM-Assisted HLS Code Tasks. NL = Natural Language, AST = Abstract Syntax Tree.

Method	Task	Input	LLM Strategy	Goal
HLS-Pilot [27]	HLS Code Optimization	C/HLS-C	Prompt Engineering	QoR
RALAD [12]	HLS Code Optimization	HLS-C	RAG	QoR
C2HLSC [17]	HLS Code Optimization	C	Prompt Engineering	Functional, QoR
SynthAI [24]	HLS Code Generation	Spec	Multi-Agent	Functional
Gai et al. [9]	HLS Code Generation	NL	Fine-tuning	Functional
SAGE-HLS [16]	HLS Code Generation	NL+AST	Fine-tuning	Functional
HLS-Seek	HLS Code Generation	NL	Fine-tuning Uncertainty-aware proxy reward	Functional, QoR

a Siamese comparative reward model that provides fast pairwise QoR ranking, and an uncertainty-aware MC dropout switching mechanism that online updates the proxy with real synthesis.

- **HLS-Seek** achieves 81.5% syntax correctness pass@1 and 81.4% Func@5 on HLS-eval with only 7B parameters, surpassing GPT-5.1 and other frontier models. On QoR evaluation, **HLS-Seek** achieves the lowest latency on 16/30 kernels, Pareto-dominates SAGE-HLS on 5 kernels and Gai et al. on 4 kernels with only 1 reverse, and demonstrates algorithmic code restructuring beyond pragma insertion.

2 Background and Motivation

As summarized in Table 1, LLM-based HLS research falls into two categories: *HLS code optimization* and *HLS code generation*.

HLS Code Optimization. These methods take existing C source code as input and apply LLMs to pragma insertion or design transformation for improved QoR. HLS-Pilot [27] uses prompt engineering to integrate profiling and pipeline optimization; RALAD [12] employs RAG to retrieve relevant optimization strategies for pragma insertion; and C2HLSC [17] iteratively refactors software C into HLS-synthesizable code via prompt engineering. While effective in their target scenarios, these inference-time strategies rely on the availability of correct C source code and do not improve the underlying model’s generative capability.

HLS Code Generation. These methods target direct code generation from natural language or high-level specifications. SynthAI [24] applies multi-agent reasoning frameworks to automate the generation pipeline from specifications. Gai et al. [9] and SAGE-HLS [16] fine-tune code LLMs on HLS datasets to produce synthesizable code from natural language descriptions.

However, as Table 1 shows, existing HLS code generation methods target only functional correctness, while HLS code optimization methods rely on prompt engineering or RAG without learning QoR-aware representations. None of these approaches trains the model with QoR feedback to jointly optimize functional correctness, latency, and resource usage. Our work fills this gap by introducing

¹https://anonymous.4open.science/r/HLS_code_generations-057E

uncertainty-aware proxy reward-based RL that enables QoR-aware training without synthesis-in-the-loop.

3 Methods

3.1 Overall Methods

Figure 2 illustrates the HLS-Seek framework. We first prepare training data via Bayesian DSE [21] with Pareto-non-dominated selection and reasoning traces from commercial models. The LLM is then trained in three stages: diversity-oriented SFT, cold-start SFT on high-quality Pareto-proximal data, and GRPO [25] with a proxy reward combining reasoning format, compilation, functional correctness, and predicted QoR (Section 3.3). The QoR reward is provided by a comparative reward model trained on offline synthesis pairs. During GRPO, MC dropout uncertainty estimation triggers selective fallback to real Vitis HLS synthesis for low-confidence candidates, with results fed back to online update the proxy, keeping synthesis overhead below 5% at convergence.

3.2 Data Preparation

Design Space Identification via Clang AST. Each HLS kernel is parsed with the Clang frontend to extract loop nests (for unrolling and pipelining) and array declarations (for partitioning strategies), constructing a kernel-specific pragma configuration space. Since this space grows exponentially, we use Bayesian optimization for efficient exploration.

HLS Corpus via Bayesian DSE. Given \mathcal{P} , we apply multi-objective Bayesian optimization with Expected Hypervolume Improvement (EHVI) to efficiently explore the design space [21]. After K iterations, we obtain evaluated configurations with their synthesis-measured QoR across five dimensions (Latency, LUT, DSP, BRAM, FF). The complete DSE dataset is preserved for diversity-oriented SFT. To facilitate cold-start reasoning training aimed at superior QoR, we isolate Pareto-non-dominated designs, ensuring the model learns from configurations that represent optimal trade-offs across all hardware metrics.

Pareto-Proximal Quality-Diversity Sampling. Retaining only the Pareto front \mathcal{F} yields too few training examples per kernel—often as few as 3–5 designs—which limits the LLM’s ability to learn fine-grained resource–latency trade-offs. We therefore construct the training set using a two-tier selection strategy. *First*, all Pareto-optimal designs are included. *Second*, for each kernel, we augment with up to K_{near} near-Pareto designs selected via a two-step process: (i) rank non-dominated designs by their normalized Euclidean distance to the Pareto front in the 5-dimensional objective space,

$$d(\mathbf{p}) = \min_{\mathbf{p}^* \in \mathcal{F}} \left\| \frac{f(\mathbf{p}) - f(\mathbf{p}^*)}{f_{\max} - f_{\min}} \right\|_2, \quad (1)$$

where f_{\max} and f_{\min} are the per-metric maximum and minimum across all evaluated designs; (ii) apply greedy farthest-point sampling among the top-ranked candidates (those with $d(\mathbf{p}) < \epsilon$) to maximize diversity in the design space. This yields a training corpus that balances *quality* (proximity to the Pareto front) and *diversity* (coverage of different resource–latency trade-off regions), providing the LLM with a richer set of competitive design alternatives per kernel.

Reasoning Traces for Cold-Start SFT. To bootstrap hardware-aware reasoning, we construct a cold-start SFT dataset of *reasoning traces*. For each natural language specification x , we query a commercial reasoning model (GPT-o1) to produce a chain-of-thought trace t that articulates step-by-step pragma selection rationale. The resulting dataset $\mathcal{D}_{\text{SFT}} = \{(x_i, t_i, y_i)\}_{i=1}^N$ pairs each specification with a reasoning trace and the corresponding HLS implementation, ensuring the base model acquires structured hardware reasoning before RL.

3.3 LLM Training with Proxy Reward

Stage 1: Diversity-Oriented SFT. We first fine-tune the base LLM on a broad HLS corpus where inputs consist of natural language descriptions paired with target QoR specifications, and outputs are the corresponding HLS implementations. This stage prioritizes diversity over optimality by exposing the model to diverse pragmas and coding patterns. It builds a basic understanding of HLS syntax and specification mapping, forming a solid foundation for later QoR-focused training.

Stage 2: Cold-Start SFT on High-Quality Data. Starting from the diversity-trained model, we perform a second round of SFT on the high-quality dataset obtained via Pareto-Proximal Quality-Diversity Sampling (Section 3.2). This dataset $\mathcal{D}_{\text{SFT}} = \{(x_i, t_i, y_i)\}_{i=1}^N$ pairs each specification with a reasoning trace and a QoR-competitive HLS implementation drawn from or near the Pareto front. Training on this curated corpus sharpens the model’s ability to generate hardware-efficient code with structured reasoning traces, producing the SFT model.

Stage 3: GRPO-based RL. Starting from the SFT model, we apply GRPO [25]. For each prompt x , we sample G candidates $\{a_i\}_{i=1}^G \sim \pi_\theta(\cdot|x)$. Each candidate receives a four-component proxy reward:

$$r(a_i) = \lambda_f r_f(a_i) + \lambda_{\text{comp}} r_{\text{comp}}(a_i) + \lambda_c r_c(a_i) + \lambda_q r_q(a_i). \quad (2)$$

The four reward components are designed to provide layered feedback from syntactic compliance to hardware quality:

Reasoning Format Reward (r_f): Encourages structured outputs of the form:

```
<think> ... </think> <final_code> ... </final_code>
```

where `<think>` contains chain-of-thought reasoning about pragma trade-offs and `</final_code>` contains the HLS code. This format promotes explicit internal reasoning, which prior work has shown to improve generation stability [25]. $r_f = 1$ if the output conforms; $r_f = 0$ otherwise.

Compilation Reward (r_{comp}): Encourages syntactically correct HLS-C. The generated code is passed to a C compiler (GCC); $r_{\text{comp}} = 1$ if compilation succeeds, 0 otherwise. This provides a dense, computationally cheap signal that is independent of functional or synthesis-level evaluation. Also, it check the dynamic memory allocations because these can not be synthesized.

Functional Correctness Reward (r_c): Encourages semantic correctness relative to the specification. The compiled code is executed against a predefined testbench, and r_c is defined as a strict binary reward, i.e., $r_c \in \{0, 1\}$. It yields 1 only if the implementation

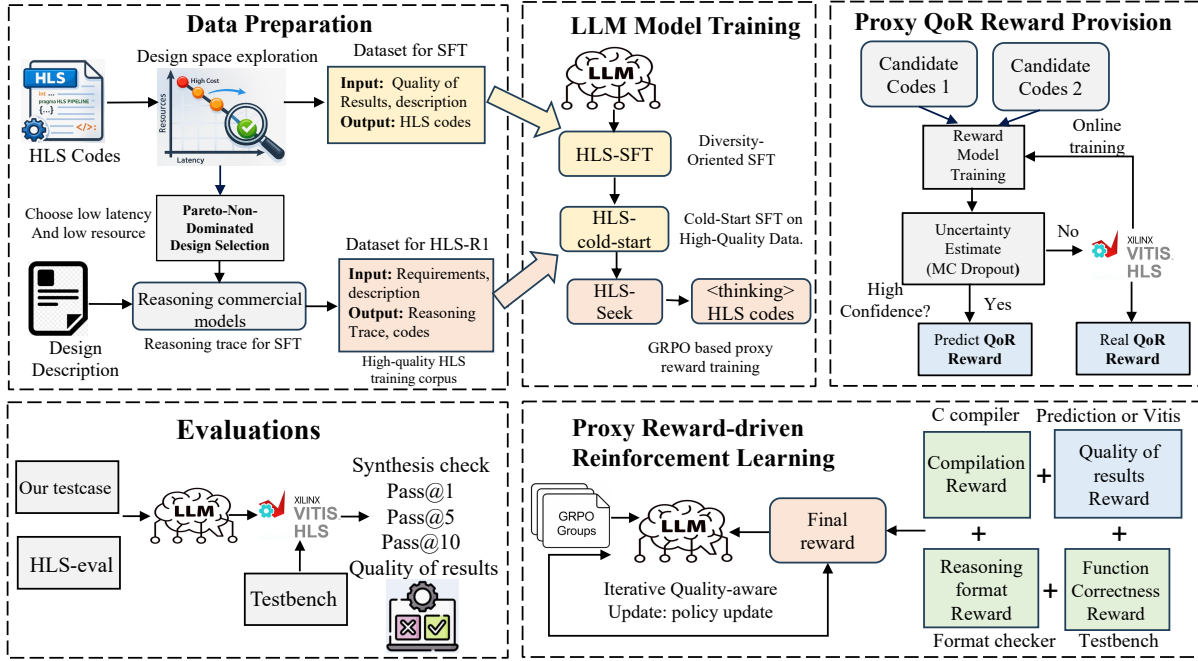


Figure 2: Overview of the HLS-Seek framework: data preparation (top-left), three-stage LLM training (top-center), proxy reward with uncertainty-aware switching (top-right), GRPO policy updates (bottom-right), and evaluation (bottom-left).

passes all test cases, and 0 otherwise, ensuring absolute functional correctness.

Proxy QoR Reward (r_q): Encourages hardware efficiency without synthesis-in-the-loop. Only candidates that pass functional testing ($r_c = 1$) are eligible. Among these, we compute r_q via *round-robin pairwise aggregation*: for each pair (i, j) of functionally correct candidates, the comparative reward model (Section 3.4) produces a soft probability $p_{ij} = P(a_i > a_j)$ via $M=10$ MC dropout forward passes. We accumulate win scores across all duels:

$$r_q(a_i) = \frac{1}{|C| - 1} \sum_{j \in C, j \neq i} p_{ij}, \quad (3)$$

where C is the set of functionally correct candidates in the group. This yields a scalar $r_q \in [0, 1]$ representing each candidate’s average win-rate, naturally converting pairwise probabilities into per-candidate QoR scores. If only one candidate passes functional testing, it receives $r_q=1.0$.

Within each group, the total rewards are normalized to group-relative advantages $\hat{A}_i = (r(a_i) - \mu_G) / (\sigma_G + \epsilon)$, and the policy is updated via the clipped surrogate loss with KL regularization. The resulting model is HLS-Seek.

3.4 Comparative Reward Model

Unlike prior HLS QoR prediction models that regress absolute values, our model performs pairwise comparison, which is simpler and directly aligned with GRPO’s relative advantage estimation. We adopt the Bradley-Terry [2] Siamese architecture (Figure 3), widely used in RLHF reward modeling [19], as it guarantees ranking transitivity and enables fast inference with a lightweight encoder.

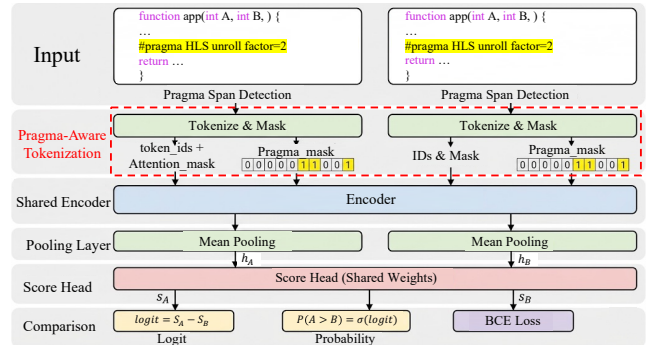


Figure 3: Architecture of the comparative reward model.

To help the model focus on the QoR-critical parts of HLS code, we introduce *Pragma-Aware Tokenization*: before encoding, we identify all `#pragma HLS` directives in the source code and prepend a special `[PRAGMA]` token to each pragma line. This allows the encoder’s attention to naturally upweight pragma regions—which govern unrolling, pipelining, and array partitioning—without modifying the underlying Transformer architecture. Each HLS design, represented as the concatenation of its functional description and pragma-annotated code, is encoded by a shared Transformer encoder with mean pooling (768-d), then mapped to a scalar score by a shared two-layer MLP (768→384→1). The preference probability is the sigmoid of the score difference, trained with BCE loss. All weights are shared between branches, ensuring ranking transitivity. We train two variants: a dominance-based ranker using pairs

where one design Pareto-dominates the other across all five PPA metrics (latency, BRAM, LUT, DSP, FF); and a latency-based ranker using pairs ordered solely by worst-case latency. Three dropout layers (rate 0.2) are retained active at inference for MC Dropout uncertainty estimation. For each application, different HLS implementations from DSE are paired and labeled with a *two-tier* scheme:

$$y_{ij} = \begin{cases} 1.0 & \text{if } i \text{ Pareto-dominates } j \text{ on all 5 QoR metrics,} \\ 0.5 & \text{if } i \text{ has strictly lower latency than } j, \\ 0.0 & \text{otherwise (tie).} \end{cases} \quad (4)$$

Full Pareto dominance ($y_{ij}=1$) captures designs that are better on every dimension, while latency-only superiority ($y_{ij}=0.5$) provides a softer signal for the common case where designs trade off latency against resource usage. Pairs with relative gap below a threshold δ are discarded to reduce label noise. Each design is mapped to a scalar score s_i via the reward model's score head. The model is trained with a combined loss:

$$\mathcal{L}_{\text{RM}} = \lambda_{\text{pair}} \mathcal{L}_{\text{BCE}}(\ell_{ij}, y_{ij}) + \lambda_{\text{cons}} \mathcal{L}_{\text{MSE}}(\ell_{ij}, s_i - s_j), \quad (5)$$

where ℓ_{ij} is the pairwise logit computed from the score difference $s_i - s_j$, and the consistency term \mathcal{L}_{MSE} regularizes the pairwise prediction to be coherent with the individual score estimates. During GRPO, only functionally correct candidates compete for QoR reranking via group-wise pairwise comparison to assign r_q . This two-tier scheme ensures that the reward model provides meaningful gradient even when full Pareto dominance is rare: latency-superior designs receive partial credit ($r_q=0.5$), while incomparable designs (same latency, different resource trade-offs) are treated as ties.

Uncertainty-Aware Proxy Reward Switching. A key risk of proxy reward models in online RL is *reward hacking*: as GRPO explores the pragma space, the policy may produce designs that exploit the reward model's out-of-distribution blind spots. To detect and mitigate this, we equip the reward model (dropout rate 0.2) with *Monte Carlo dropout uncertainty estimation* [10]. We retain dropout layers active during inference and perform $M=10$ stochastic forward passes per candidate:

$$u_i = \text{Var}_{m=1}^M [s^{(m)}(a_i)], \quad (6)$$

where $s^{(m)}(a_i)$ is the score head output under the m -th dropout mask. When $u_i > \tau_u=0.1$ for any candidate in the group, we invoke real Vitis HLS synthesis for that candidate and use the result to compute r_q . This synthesis result is added to a dynamic replay buffer \mathcal{B} , which is used to fine-tune \mathcal{M} online every $K_{\text{update}}=100$ steps (learning rate 2×10^{-6} , 50 fine-tuning steps per update). This adaptive mechanism serves two purposes: (i) it grounds rewards at policy frontier states where the proxy is least reliable, preventing reward hacking; and (ii) it continuously improves \mathcal{M} 's coverage as the policy explores new regions. By design, the proxy does not need to be accurate on out-of-distribution candidates: the MC dropout mechanism detects such cases and routes them to real synthesis, ensuring reward fidelity regardless of proxy coverage.

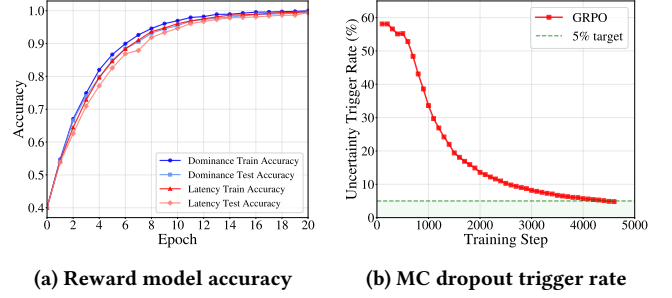


Figure 4: Evaluation of the proxy reward mechanism.

4 Experiments

4.1 Experimental Setup

Model and Hardware. All experiments use **Qwen2.5-Coder-7B-Instruct** [13] as the base model, fine-tuned on $2 \times$ NVIDIA H200 GPUs with bf16 and AdamW optimizer. HLS synthesis and QoR evaluation use **Vitis HLS 2023.1** targeting a AMD Alveo U280 FPGA (xcu280-fsvh2892-2L-e, Virtex UltraScale+ HBM) with a clock period of 10 ns (100 MHz). Frontier model baselines (GPT-5.1, DeepSeek-V3.2, Gemini-3-Pro, Qwen3-235B) are accessed via the ChatFire API² with temperature 0.7 and default decoding settings.

Dataset. Training data is aggregated from three open-source HLS datasets: ForgeHLS [21], SAGE-HLS [16], and HLStrans [30], comprising a total of 12,661 applications and 450,273 samples. The diversity-oriented SFT (Stage 1) uses the remaining applications with QoR descriptions for broad pragma coverage. The cold-start SFT (Stage 2) selects 418 applications and applies our Pareto-Proximal Quality-Diversity Sampling to curate high-quality samples paired with reasoning traces. GRPO training (Stage 3) uses 1,013 applications. The comparative reward model is trained on pairwise examples from DSE-generated HLS variants across all datasets. Evaluation is conducted on the independent HLS-eval [9] benchmark (43 kernels) and a randomly selected ForgeHLS test set (108 applications), with no overlap between training and evaluation data.

SFT Training. Both SFT stages apply LoRA fine-tuning with rank $r=64$, scaling $\alpha=128$, and dropout 0.05, targeting the projection and FFN modules in transformer block. Each stage is trained for 3 epochs with a learning rate of 2×10^{-4} , batch size 16, and gradient checkpointing enabled.

GRPO Training. Starting from the SFT checkpoint, GRPO uses group size $G=4$, learning rate 5×10^{-7} , clip ratio $\epsilon=0.2$, KL coefficient $\beta=0.02$, and 2 PPO epochs per batch. Generation employs temperature 0.9, top- p 0.95, and a maximum of 2,048 new tokens.

Comparative Reward Model. The pairwise reward model is built on **UniXcoder-base** [11], fine-tuned for 20 epochs with learning rate 1×10^{-5} , batch size 16, and dropout 0.2. The maximum input length is set to cover the full code length of all kernels in the dataset. Pairs with relative QoR difference below 10% are discarded to reduce label noise. The combined loss weights pairwise ranking and consistency regularization as $\lambda_{\text{pair}}=1.0$ and $\lambda_{\text{cons}}=0.5$.

²<https://api.chatfire.cn/>

Table 2: Evaluation results on ForgeHLS test set (108 apps) and the independent HLS-eval benchmark (Higher is better).

Type	Model	Size	ForgeHLS Test Set (%)						HLS-eval (%)			
			Syntax Correctness			Functional Correctness			Syntax Corr.		Func. Corr.	
			pass@1	pass@5	pass@10	pass@1	pass@5	pass@10	pass@1	pass@5	pass@1	pass@5
Foundational Models	GPT-5.1	-	84.3	<u>89.8</u>	<u>91.7</u>	73.1	<u>80.6</u>	<u>82.4</u>	91.7	97.7	71.7	<u>79.1</u>
	DeepSeek-V3.2	-	73.1	88.0	89.8	62.0	77.8	80.6	77.3	93.0	51.9	65.1
	Gemini-3-Pro	-	62.0	88.0	90.7	55.6	78.7	80.6	67.1	<u>95.3</u>	55.9	<u>79.1</u>
	Qwen3-235B	235B	33.3	42.6	43.5	24.1	37.0	39.8	61.8	79.1	43.9	67.4
Code Models	Qwen2.5-Coder	32B	75.0	86.1	87.0	61.1	75.9	75.9	77.0	88.4	46.8	58.1
	Qwen2.5-Coder	14B	77.8	86.1	87.0	63.9	76.9	77.8	73.6	81.4	36.7	44.2
	DeepSeek-Coder	6.7B	63.9	86.1	88.0	46.3	74.1	78.7	69.0	93.0	29.1	46.5
	Qwen2.5-Coder	7B	41.7	76.9	82.4	24.1	63.0	69.4	45.4	83.7	16.0	41.9
	CodeLlama	7B	17.6	57.4	75.0	10.2	38.0	52.8	19.3	62.8	10.6	39.5
	StarCoder2	15B	19.4	31.5	49.1	8.1	13.9	24.1	8.6	41.9	4.8	34.9
Gai et al. [9]	CodeLlama	7B	22.2	28.7	45.4	15.7	17.6	27.8	6.3	48.8	1.4	27.9
SAGE-HLS [16]	Qwen2.5-Coder	7B	77.8	88.0	88.0	63.9	76.9	77.8	67.8	76.7	34.8	41.9
Ours	HLS-Seek (SFT)	7B	78.7	89.8	90.7	66.7	79.6	82.4	77.5	88.4	50.7	60.5
	HLS-Seek (GRPO)	7B	<u>81.5</u>	91.7	93.5	<u>71.3</u>	84.3	87.0	<u>84.7</u>	<u>95.3</u>	<u>68.9</u>	81.4

4.2 Evaluation Metrics and Benchmarks

Syntax Correctness. We measure *syntax correctness* as the compilation pass rate—the fraction of generated HLS programs that successfully pass Vitis HLS compilation without syntax or type errors. A design that fails to compile cannot be synthesized or tested, so this metric captures the fundamental quality bar for HLS code generation.

Functional Correctness. We report functional correctness using the $\text{pass}@k$ metric [3], which estimates the probability that at least one correct solution appears in k independent samples. Correctness is determined by running the generated HLS code against provided testbenches. We report $\text{pass}@1$, $\text{pass}@5$, and $\text{pass}@10$.

QoR-Aware Evaluation. Beyond functional correctness, we evaluate whether LLMs can generate HLS code that is also hardware-efficient. We conduct a QoR-aware experiment on benchmark by appending the optimization directive “Write HLS code for least latency with least resource” to each prompt, instructing the model to simultaneously minimize execution latency (cycles) and resource usage (LUT, DSP, BRAM, FF). We sample N candidates, filter for functional correctness, synthesize all passing designs with Vitis HLS, and compare the resulting QoR against reference designs using Pareto dominance.

Data Independence. To ensure no data leakage between training and evaluation, we verify separation via MD5 hash deduplication on every training and evaluation record, using both raw hashes and a normalized form (comments and whitespace stripped). Across all train-eval splits (SFT/GRPO training vs. ForgeHLS test set, and vs. HLS-eval), we observe zero exact and zero normalized matches.

4.3 Main Results

4.3.1 Proxy Reward Effects. The proxy reward model only needs to serve GRPO training, which covers 1,013 applications. It is trained

on 398,734 pairwise samples constructed from DSE-generated HLS variants of these applications. Crucially, the task is *graded pairwise comparison*—the model predicts whether design A is better than B via Pareto dominance (score 1.0) or latency superiority (score 0.5), rather than predicting absolute resource or latency values. This relative comparison is inherently easier than regression, as the two-tier labels produce clear margins between quality levels. As shown in Figure 4a, both the dominance and latency variants converge above 99% by epoch 20 with minimal train-test gap, indicating no overfitting. The final test accuracy reaches **99.53%** for Pareto-dominance and **99.42%** for latency-only comparison, confirming that both tiers of the reward signal are reliably predicted.

Figure 4 (right) shows the MC dropout uncertainty trigger rate during GRPO training. Early in training, over 55% of candidates trigger real Vitis HLS synthesis due to high reward model uncertainty on the policy’s out-of-distribution outputs. As training progresses and the reward model is updated with synthesis results, the trigger rate decreases monotonically, dropping below the 5% target after approximately 4,500 steps. This confirms that the uncertainty-aware switching mechanism is self-correcting: it grounds rewards when most needed (early training) while adding negligible overhead at convergence.

4.3.2 HLS Code Generation Results. Table 2 reports syntax correctness and functional correctness across all baselines. Our proposed, **HLS-Seek**, consistently achieves the best results at the 7B parameter and outperforms models that are orders of magnitude larger.

Syntax Correctness. HLS-Seek achieves **81.5%** $\text{pass}@1$ syntax correctness, surpassing all code-specialist baselines despite only 7B parameters. At $\text{pass}@5$ and $\text{pass}@10$ it reaches **91.7%** and **93.5%**, the highest values in the table, indicating the model rarely fails to produce a compilable design within a small sample budget. Among

Table 3: QoR comparison on all functionally correct kernels. “–” indicates synthesis failure or timeout. Bold = lowest latency or Pareto-dominant entry.

Kernel	SAGE-HLS [16] (Lat./DSP/FF/BRAM/LUT)	Gai et al. [9] (Lat./DSP/FF/BRAM/LUT)	GPT-5.1 (Lat./DSP/FF/BRAM/LUT)	HLS-Seek (Lat./DSP/FF/BRAM/LUT)
fgnn_linear	554/5/3305/1/4791	–	169/12/5730/0/2864	116/648/90762/0/67419
block_freq	529/11/1290/0/1289	529/11/1290/0/1289	161/11/3419/4/4717	161/11/3419/4/4717
global_add_pool	18/2/3150/2/2533	18/2/404/0/660	1626/2/606/0/1164	10/16/8816/0/5906
gemver	8252/11/5399/4/5285	2617/33/27898/0/8646	8042/22/2967/0/3202	1938/44/52621/0/17716
seidel_2d	758521/3/1222/0/1732	61073/24/17611/0/11468	758521/3/1222/0/1732	1099761/3/829/0/1367
spam_dotProduct	1152/64/1409/0/5746	1026/2/46/0/171	36/64/1042/0/3705	132/16/1782/0/2660
max_widen_port	81/0/1158/2/1235	130/0/17/0/109	81/0/1787/4/2001	129/0/19/0/117
data_forwarding [†]	1024/0/1025/0/2715	1026/0/25/0/77	1040/0/1889/4/1962	514/0/309/0/638
hamming_encoder	512/0/513/0/31139	1026/0/25/0/99	1026/0/25/0/105	514/0/23/0/129
instr_pipeline	1023/0/1024/0/45344	1026/0/25/0/116	1028/0/29/0/116	641/0/118/0/810
mag_comparator	1026/0/303/4/402	2050/0/25/0/117	1026/0/25/0/116	1026/0/25/0/190
comparator_8bit [†]	2063/0/12356/2/22019	1026/0/25/0/115	1041/0/2555/6/3089	514/0/25/0/450
mux_4_to_1	–	2074/0/2383/2/2451	1027/0/42/0/103	515/0/64/0/1296
nand_gate	512/0/513/0/28333	3086/0/112/0/34639	1026/0/25/0/81	514/0/23/0/85
pll_2x	1026/0/24/0/120	–	1028/0/29/0/77	514/0/36/0/213
pll_8x	512/0/513/0/18851	2050/0/25/0/78	1026/0/25/0/77	1025/0/36/0/85
xor_gate	512/0/513/0/26285	2050/0/372/0/486	4/0/15/0/1082	1026/0/27/0/131
karaoke_proc	1045/8/1833/2/1756	–	1031/8/801/0/668	263/32/2288/0/1879
video_proc	1048578/0/262/8/425	1048578/0/66/0/245	1048580/0/70/0/245	262401/0/19515/0/63162
binary_counter	–	1030/0/851/0/929	512/0/513/0/335267	518/0/1666/0/1810
hs_6bit_adder [†]	512/0/513/0/18877	–	1041/0/2526/6/3047	514/0/36/0/239
ittyBittyComp	1026/0/24/0/98	2060/0/2060/5/2501	1026/0/91/0/216	258/0/343/0/1187
periph_interface	1026/0/61/0/165	1026/0/25/0/116	1026/0/25/0/116	1026/0/25/0/136
video_ctrl	–	–	2073606/0/220/0/322	2073606/0/220/0/322
crc32	1027/0/291/2/2342	–	1027/0/81/0/2211	11265/0/64/0/428
digital_phase	1051/42/2943/0/7452	1060/42/3023/0/7535	1049/32/2321/0/9060	1049/32/2321/0/9060
hazard_detect	–	–	1026/0/25/0/297	514/0/437/0/3717
portfolio_opt	–	–	23408932/11/2053/0/2479	318983060/19/2771/4/2817
vector_add	1026/0/301/6/366	–	1026/0/25/0/116	514/0/369/0/679

Lowest latency: HLS-Seek 16/30, GPT-5.1 9/30, SAGE-HLS 6/30, Gai et al. 1/30
Pareto Dominance. (HLS-Seek wins/loses): vs SAGE-HLS 5/0, vs Gai 4/1, vs GPT-5.1 3/3

foundational models, GPT-5.1 (84.3%) achieves higher pass@1 but falls behind at pass@5 (89.8%) and pass@10 (91.7%). Compared with the HLS-specific baseline SAGE-HLS (77.8%), HLS-Seek achieves a +3.7 pp gain at pass@1 and +3.7 pp at pass@5, confirming the benefit of QoR-aware reinforcement learning.

Functional Correctness. HLS-Seek achieves 71.3% functional pass@1, and its advantage becomes decisive at higher sample budgets: **84.3%** pass@5 and **87.0%** pass@10, the highest values in the table, outperforming GPT-5.1 by +3.7 pp and +4.6 pp respectively. Among code models, Qwen2.5-Coder-14B (63.9%) and DeepSeek-Coder-6.7B (46.3%) achieve competitive pass@1 but lag significantly at higher budgets. Notably, general code models such as StarCoder2-15B achieve low syntax correctness (6.5% pass@1) and low functional correctness (1.9%), illustrating that HLS-specific training is necessary for semantically correct kernel generation.

HLS-eval Benchmark. On the cross-benchmark HLS-eval task, HLS-Seek achieves **84.7%** Syntax pass@1 / **95.3%** pass@5 and **68.9%** Func pass@1 / **81.4%** pass@5. While GPT-5.1 achieves higher Syntax pass@5 (97.7%), HLS-Seek surpasses it on Func pass@5 by +2.3 pp (81.4% vs. 79.1%). Compared with SAGE-HLS (67.8% / 76.7% Syntax, 34.8% / 41.9% Func), HLS-Seek achieves substantial gains across all metrics (+16.9 pp Syntax pass@1, +18.6 pp Syntax pass@5, +34.1 pp Func pass@1, +39.5 pp Func pass@5), confirming the effectiveness of proxy reward-based reinforcement learning.

4.3.3 Quality of Results. Table 3 reports post-synthesis QoR (Latency/DSP/FF/BRAM/LUT) for kernels where all four models produce functionally correct and synthesizable designs. We select these kernels from both the HLS-eval benchmark and our ForgeHLS test

set (108 applications). Among commercial models, we choose GPT-5.1 as the representative baseline because it achieves the highest functional correctness in Table 2. The two HLS-specific baselines are SAGE-HLS [16] and Gai et al. [9]. All models are prompted with “Write HLS code for least latency with least resource” to elicit QoR-optimized outputs. For each kernel, we sample 5 candidates per model and report the QoR of the best functionally correct design (best-of-5), consistent with the pass@5 protocol in Table 2.

Latency. HLS-Seek achieves the lowest latency on the majority of kernels. On compute-intensive designs such as gemver (1938 vs. 8042 for GPT-5.1), video_proc (262401 vs. 1048580), and karaoke_proc (263 vs. 1031), HLS-Seek reduces latency by 2–4× compared to all baselines. This advantage stems from the QoR-aware GRPO training, which rewards aggressive pragma strategies (e.g., loop unrolling, pipelining) that reduce execution cycles.

Resource Trade-off. The latency reduction often comes at the cost of higher resource usage. For example, on fgnn_linear, HLS-Seek achieves the lowest latency (116) but uses significantly more FF and LUT than GPT-5.1. Conversely, on simpler kernels such as comparator_8bit and data_forwarding, HLS-Seek achieves both lower latency and moderate resource consumption, demonstrating that the model can identify efficient pragma configurations when the design space permits.

Pareto Dominance. Considering all five QoR dimensions simultaneously, HLS-Seek Pareto-dominates SAGE-HLS on 5 kernels with 0 reverse, [9] on 4 kernels with 1 reverse, and GPT-5.1 on 3 kernels with 3 reverse. The clear advantage over HLS-specific baselines (9:1 aggregate) confirms that QoR-aware RL training produces designs

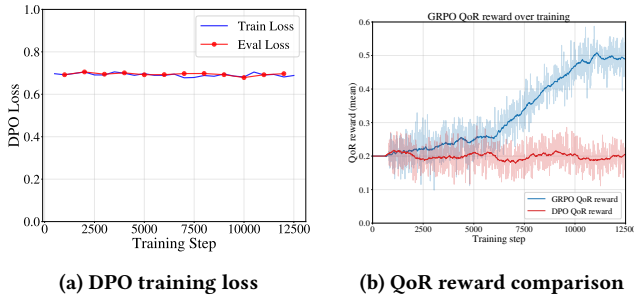


Figure 5: DPO training loss and QoR reward comparison.

that are not merely faster but holistically better across resource dimensions. Against GPT-5.1, the symmetric 3:3 result reflects a natural trade-off: HLS-Seek favors latency-optimized designs while GPT-5.1 tends toward resource-conservative configurations.

Comparison with Baselines. [9] frequently fails synthesis or times out, reflecting the limited pragma awareness of its CodeLlama-based fine-tuning. SAGE-HLS produces conservative designs with moderate latency but occasionally incurs extremely high LUT usage (e.g., `nand_gate`: 28333 LUT, `hamming_encoder`: 31139 LUT). GPT-5.1 generates resource-efficient code but tends toward conservative pragma usage, resulting in higher latency on most kernels.

4.4 Ablation Study

Training Strategy. PPaRTL [29] applies Direct Preference Optimization (DPO) for QoR-aware RTL generation. We evaluate whether DPO can similarly improve HLS code quality. Figure 5 contrasts DPO and our GRPO training dynamics. DPO preference pairs are constructed from the same 1,013 applications used for GRPO, each with multiple design variants synthesized with different HLS pragma configurations and annotated with real PPA metrics (latency, BRAM, LUT, DSP, FF) from Vitis HLS. For each application, we pair the lowest-latency design (chosen) against the highest-latency design (rejected), yielding strong preference signals with large quality gaps. Despite this favorable setup, the DPO loss plateaus around 0.693 (close to $\ln 2$, the random-guess baseline for binary cross-entropy), indicating that DPO fails to learn meaningful preferences between HLS designs. This confirms the limitation, pragma-level differences produce minimal token-level distances that preference learning cannot distinguish. For fair comparison, Figure 5b evaluates both DPO and GRPO checkpoints using the same QoR reward computation (round-robin pairwise r_q via the proxy reward model). The DPO-trained model’s QoR reward remains flat at ~ 0.2 throughout, confirming that DPO fails to improve hardware quality. In contrast, GRPO’s QoR reward rises steadily from 0.2 to ~ 0.5 , demonstrating that the proxy reward provides effective learning signals that drive continuous QoR improvement. **Real Reward vs. Proxy Reward GRPO.** To further demonstrate the effectiveness of our proposed proxy reward, we compare it against real synthesis-based reward, which uses synthesis QoR as a reinforcement learning signal, representing a state-of-the-art approach in RTL code generation (e.g., ChipSeek-R1 [6]). Specifically, we show that this approach is impractical for training high-quality

HLS code generation models, as EDA synthesis becomes the dominant bottleneck in the training loop. Table 4 compares GRPO with full Vitis HLS synthesis (Real Reward) against our proxy reward approach on both training cost and final QoR. Under the same 73-hour wall-clock budget, proxy reward completes 12,500 GRPO steps (8.8 s/step for proxy inference plus ~ 42 hours of selective synthesis fallback triggered by MC dropout uncertainty), while real reward completes only 1,460 steps at 180 s/step. The QoR gap is decisive: Proxy achieves 16/30 lowest-latency kernels and 9 Pareto-dominance wins, versus just 3/30 and 2 for Real Reward. Note that completing all 12,500 steps with real reward would require ~ 26 days of wall-clock time, making full synthesis-in-the-loop RL impractical.

4.5 Case Study

We illustrate HLS-Seek’s advantage through a case study on Poly-Bench GEMVER (Figure 6), a BLAS matrix-vector computation with $N=40$ and double precision. GPT-5.1 generates a fused loop with a scalar accumulator—functionally correct but inherently serial, as the scalar cannot be partitioned for parallel memory access. It applies only PIPELINE II=1 on the innermost loop with no array partitioning, yielding low resource usage (22 DSP, 3,202 LUT) but high latency (8,042 cycles). Stage 2, which requires column-wise access to $A(A[j][i])$, suffers memory conflicts that inflate its latency to $\sim 3,214$ cycles. HLS-Seek learns to apply *scalar expansion* and *loop fission*: replacing `double acc` with `double tmp1[40]` and splitting the loop into independent accumulation and assignment phases. The array form enables ARRAY_PARTITION for parallel bank access, while loop fission allows independent scheduling of each phase. Combined with UNROLL factor=2 on both loop levels, these transformations yield a **4.1 \times** overall latency reduction (8,042 \rightarrow 1,938 cycles) at the cost of 5.5 \times LUT overhead (3,202 \rightarrow 17,716). Notably, this is not mere pragma insertion but *algorithmic restructuring*—an optimization pattern that HLS-Seek discovers through reinforcement learning with QoR-aware reward signals. This demonstrates that beyond pragma optimization, HLS-Seek can learn to transform code structure itself to unlock hardware parallelism that is inaccessible to pragma-only approaches.

5 Conclusion

We presented HLS-Seek, a QoR-aware framework for NL-to-HLS code generation that combines a three-stage training pipeline with GRPO-based reinforcement learning and a comparative reward model. The uncertainty-aware proxy reward switching mechanism enables online self-improvement of the reward model, achieving 8.5 \times training speedup over synthesis-in-the-loop RL while matching its final performance. HLS-Seek achieves 81.5% syntax correctness pass@1 and 81.4% Func@5 on HLS-eval with only 7B parameters, outperforming GPT-5.1 and other frontier models at

Table 4: Training cost and QoR comparison: Synthesis-in-the-loop vs. HLS-Seek.

Method	Time/step	Wall-clock	Steps	Low. Lat.	Pareto
Real Reward	180 s	73h	1,460	3/30	2
Proxy (Ours)	8.8 s + fallback	73h	12,500	16/30	9

GPT-5.1 (3,214 cycles)	HLS-Seek (507 cycles, 6.3x)
<pre>// Fused: accumulate + assign for (int i = 0; i < 40; i++) { double acc = 0.0; for (int j = 0; j < 40; j++) { #pragma HLS PIPELINE II=1 acc += A[j][i] * y[j]; } x[i] = beta * acc + z[i]; }</pre>	<pre>// Split 1: accumulate into array double tmp1[40] = {0}; for (int i = 0; i < 40; i++) { for (int j = 0; j < 40; j++) { #pragma HLS UNROLL factor=2 tmp1[i] += A[j][i] * y[j]; } } // Split 2: assign for (int i = 0; i < 40; i++) x[i] = beta * tmp1[i] + z[i];</pre>

Figure 6: Key code snippets of GEMVER.

higher sample budgets. On QoR evaluation, HLS-Seek consistently produces lower-latency designs by learning aggressive pragma strategies and algorithmic restructuring that general-purpose LLMs cannot discover. Our results demonstrate that domain-specific RL with learned QoR rewards is a viable path toward fully automated, hardware-efficient HLS code generation.

Acknowledgments

References

- [1] Gustavo Alonso, Timothy Roscoe, David Cock, Mohsen Ewaida, Kaan Kara, Dario Korolija, David Sidler, and Zeke Wang. 2020. Tackling Hardware/Software co-design from a database perspective. In *10th Annual Conference on Innovative Data Systems Research (CIDR 2020), Online Proceedings*. CIDR, CIDR, Amsterdam, Netherlands, 30.
- [2] Ralph Allan Bradley and Milton E Terry. 1952. Rank analysis of incomplete block designs: I. the method of paired comparisons. *Biometrika* 39, 3/4 (1952), 324–345.
- [3] Mark Chen, Jerry Tworek, Heewoo Jun, Qiming Yuan, Henrique Ponde De Oliveira Pinto, Jared Kaplan, Harri Edwards, Yuri Burda, Nicholas Joseph, Greg Brockman, et al. 2021. Evaluating large language models trained on code. *arXiv preprint arXiv:2107.03374* abs/2107.03374 (2021), 1–34.
- [4] Xinyu Chen, Hongshi Tan, Yao Chen, Bingsheng He, Weng-Fai Wong, and Deming Chen. 2021. ThunderGP: HLS-based Graph Processing Framework on FPGAs. In *The 2021 ACM/SIGDA International Symposium on Field-Programmable Gate Arrays*. ACM, Virtual Event, USA, 69–80.
- [5] Yao Chen, Jiong He, Xiaofan Zhang, Cong Hao, and Deming Chen. 2019. Cloud-DNN: An open framework for mapping DNN models to cloud FPGAs. In *Proceedings of the 2019 ACM/SIGDA international symposium on field-programmable gate arrays*. ACM, Seaside, CA, USA, 73–82.
- [6] Zhirong Chen, Kaiyan Chang, Zhuolin Li, Xinyang He, Chujie Chen, Cangyuan Li, Mengdi Wang, Haobo Xu, Yinhe Han, and Ying Wang. 2025. Chipseeker1: Generating human-surpassing rtl with llm via hierarchical reward-driven reinforcement learning. *arXiv preprint arXiv:2507.04736* abs/2507.04736 (2025), 1–15.
- [7] Guohao Dai, Tianhao Huang, Yuze Chi, Ningyi Xu, Yu Wang, and Huazhong Yang. 2017. Foregraph: Exploring large-scale graph processing on multi-FPGA architecture. In *Proceedings of the 2017 ACM/SIGDA International Symposium on Field-Programmable Gate Arrays*. ACM, Monterey, CA, USA, 217–226.
- [8] Javier Duarte et al. 2018. Fast Inference of Deep Neural Networks in FPGAs for Particle Physics. *Journal of Instrumentation* 13, 07 (2018), P07027.
- [9] Jiahao Gai, Hao Chen, Zhican Wang, Hongyu Zhou, Wanru Zhao, Nicholas Lane, and Hongxiang Fan. 2025. Exploring code language models for automated hls-based hardware generation: Benchmark, infrastructure and analysis. In *Proceedings of the 30th Asia and South Pacific Design Automation Conference*. ACM, Tokyo, Japan, 988–994.
- [10] Yarin Gal and Zoubin Ghahramani. 2016. Dropout as a Bayesian Approximation: Representing Model Uncertainty in Deep Learning. In *Proceedings of the 33rd International Conference on Machine Learning (ICML)*. JMLR.org, New York, NY, USA, 1050–1059.
- [11] Daya Guo, Shuai Lu, Nan Duan, Yanlin Wang, Ming Zhou, and Jian Yin. 2022. Unixcoder: Unified cross-modal pre-training for code representation. In *Proceedings of the 60th Annual Meeting of the Association for Computational Linguistics (Volume 1: Long Papers)*. ACL, Dublin, Ireland, 7212–7225.
- [12] H. Xu et al. 2024. Optimizing High-Level Synthesis Designs with Retrieval-Augmented Large Language Models. In *2024 IEEE LLM Aided Design Workshop (LAD)*. IEEE, IEEE, San Francisco, CA, USA, 1–5.
- [13] Binyuan Hui, Jian Yang, Zeyu Cui, Jiayi Yang, Dayiheng Liu, Lei Zhang, Tianyu Liu, Jiajun Zhang, Bowen Yu, Keming Lu, et al. 2024. Qwen2.5-coder technical report. *arXiv preprint arXiv:2409.12186* abs/2409.12186 (2024), 1–29.
- [14] J. Cong et al. 2022. FPGA HLS today: successes, challenges, and opportunities. *ACM Transactions on Reconfigurable Technology and Systems (TRETS)* 15, 4 (2022), 1–42.
- [15] Wenqi Jiang, Dario Korolija, and Gustavo Alonso. 2023. Data processing with fpgas on modern architectures. In *Companion of the 2023 International Conference on Management of Data*. ACM, Seattle, WA, USA, 77–82.
- [16] M. Zafir Sadik Khan, Nowfel Mashnoor, Mohammad Akyash, Kimia Zamiri Azar, and Hadi Mardani Kamali. 2025. SAGE-HLS: Syntax-Aware AST-Guided LLM for High-Level Synthesis Code Generation. In *43rd IEEE International Conference on Computer Design, ICCD 2025, Richardson, TX, USA, November 10-12, 2025*. IEEE, 574–581. doi:10.1109/ICCD65941.2025.00088
- [17] L. Collini et al. 2024. C2HLS: Can LLMs Bridge the Software-to-Hardware Design Gap?. In *2024 IEEE LLM Aided Design Workshop (LAD)*. IEEE, IEEE, San Francisco, CA, USA, 1–12.
- [18] Rene Mueller, Jens Teubner, and Gustavo Alonso. 2009. Data processing on FPGAs. *Proceedings of the VLDB Endowment* 2, 1 (2009), 910–921.
- [19] Long Ouyang, Jeffrey Wu, Xu Jiang, Diogo Almeida, Carroll Wainwright, Pamela Mishkin, Chong Zhang, Sandhini Agarwal, Katarina Slama, Alex Ray, et al. 2022. Training language models to follow instructions with human feedback. *Advances in neural information processing systems* 35 (2022), 27730–27744.
- [20] P. Coussey et al. 2010. *High-level synthesis*. Vol. 1. Springer, Dordrecht, Netherlands.
- [21] Zedong Peng, Zeju Li, Mingzhe Gao, Qiang Xu, Chen Zhang, and Jieru Zhao. 2025. ForgeHLS: A Large-Scale, Open-Source Dataset for High-Level Synthesis. *arXiv preprint arXiv:2507.03255* abs/2507.03255 (2025), 1–15.
- [22] S. Lahti et al. 2018. Are we there yet? A study on the state of high-level synthesis. *IEEE Transactions on Computer-Aided Design of Integrated Circuits and Systems* 38, 5 (2018), 898–911.
- [23] S. Swaroopa et al. 2024. Evaluating Large Language Models for Automatic Register Transfer Logic Generation via High-Level Synthesis. *arXiv preprint arXiv:2408.02793* abs/2408.02793 (2024), 1–8.
- [24] SA. Sheikholeslam et al. 2024. SynthAI: A Multi Agent Generative AI Framework for Automated Modular HLS Design Generation. *arXiv preprint arXiv:2405.16072* abs/2405.16072 (2024), 1–10.
- [25] Zhihong Shao, Peiyi Wang, Qihao Zhu, Runxin Xu, Junxian Song, Xiao Bi, Haowei Zhang, Mingchuan Zhang, YK Li, Yu Wu, et al. 2024. DeepSeekMath: Pushing the limits of mathematical reasoning in open language models. *arXiv preprint arXiv:2402.03300* abs/2402.03300 (2024), 1–29.
- [26] Hongshi Tan, Xinyu Chen, Yao Chen, Bingsheng He, and Weng-Fai Wong. 2023. LightRW: Fpga accelerated graph dynamic random walks. *Proceedings of the ACM on Management of Data* 1, 1 (2023), 1–27.
- [27] X. Chenwei et al. 2024. HLSPIlot: LLM-based High-Level Synthesis. arXiv:2408.06810 [cs.AR] <https://arxiv.org/abs/2408.06810>
- [28] Shulin Zeng, Jun Liu, Guohao Dai, Xinhao Yang, Tianyu Fu, Hongyi Wang, Wenheng Ma, Hanbo Sun, Shiyao Li, Zixiao Huang, et al. 2024. FlightLLM: Efficient large language model inference with a complete mapping flow on fpgas. In *Proceedings of the 2024 ACM/SIGDA International Symposium on Field Programmable Gate Arrays*. ACM, Monterey, CA, USA, 223–234.
- [29] Yining Zhao, Susmit Jha, et al. 2025. Hardware Generation with High Flexibility using Reinforcement Learning Enhanced LLMs. In *Proceedings of the 62nd ACM/IEEE Design Automation Conference*. ACM, San Francisco, CA, USA, 1–6.
- [30] Qingyun Zou et al. 2025. HLStrans: Dataset for C-to-HLS Hardware Code Synthesis. *arXiv preprint arXiv:2507.04315* abs/2507.04315 (2025), 1–12.